Three-Level Mass-Transfer Model for the Heterogeneous Polymerization of Olefins

Pål Kittilsen,* Hallvard F. Svendsen

Department of Chemical Engineering, Norwegian University of Science and Technology (NTNU), N-7491 Trondheim, Norway

Received 18 June 2001; accepted 2 July 2003

ABSTRACT: The introduction of a mesoparticle scale can be important in the description of mass-transfer effects in the heterogeneous polymerization of olefins. Recent studies have shown that a morphological size level on the order of some tenths of the size of the whole particle exists. The use of traditional models that include mass-transfer effects only at the macro- and microscales gives conflicting results when the mass-transfer resistance at the meso level becomes significant. A new model to account for these effects is shown here. © 2003 Wiley Periodicals, Inc. J Appl Polym Sci 91: 2158–2167, 2004

Key words: single-particle modeling; polyolefins; mass transfer; morphology; heterogeneous polymers

INTRODUCTION

One important route for polymerizing olefins like ethylene and propylene is by processes using heterogeneous catalysts. The catalyst is supported on an inert carrier that provides control of the morphology of the final product and avoids fines in the reactor. In the early stages of the "life" of the catalyst/polymer particle, the catalyst goes through a breakup process, in which the catalyst carrier fragments. However, the particles normally do not disintegrate because of the entanglement of the polymer chains. Polymer continues to form around the catalyst fragments and forms what is called micrograins in standard models. Thus, the particle can be considered to consist of an agglomerate of microparticles. This is the basic particle picture of the multigrain model (MGM).[1] In the MGM, the particle is assumed to be pseudo-homogeneous on the macroscale level because the microparticles are very small with respect to the macroparticle and they are homogeneously distributed in the particle.

The model presented here introduces a third level in the description of the particle morphology. The new scale is some tenths of the macroscale. We call this the mesoscale. As shown in the work by Kittilsen and McKenna,[2] where the effect of ethylene–propylene–rubber (EPR) polymerization on particle morphology was investigated, a morphological description on the mesoscale level was necessary to describe the mass-transfer conditions. Such an approach is not new. Skomorokhov et al.[3] suggested that the microparticles as described by MGM eventually agglomerated to larger substructures in the polymer particles. Thus, the mass-transfer properties changed, and a morphology level between the macroscale and the microscale was necessary to obtain a proper mass-transfer description. The theory was supported by experimental morphology studies. Also McKenna and Schweich[4] suggested a multilevel catalyst model after studying SEM images and porosimetry curves. In their implemented model, they used three scales: micro, meso, and macro.

One of the critical factors in the works cited above is the implicit assumption of a homogeneous boundary condition around the mesoparticles (i.e., that the concentration of monomer surrounding a mesoparticle is uniform). This is probably a good approximation for small mesoparticles, as is the case in McKenna and Schweich's work. However, as the size of the mesoparticle approaches some tenths of the scale of the macroparticle, as in Skomorokhov et al.'s work, it is obvious that the concentration may vary from one side of the mesoparticle to the other. In this work we studied whether this assumption may also be valid in the case of large mesoparticles.

Recently, other studies have also experimentally revealed the need for including length scales other than the micro- and macroscales for mass transfer in polyolefin particles. Sliepcevich et al.[5] measured diffusivities in polymer particles by inverse gas chromatography. From the retention time and distribution of the monomer in the chromatograph, they could calculate the time scale, and a corresponding length scale of

Correspondence to: H. Svendsen (hallvard.svendsen@chembio.ntnu.no).

*P.K. is also affiliated with Norsk Hydro ASA, Corporate Research Centre, Porsgrunn, Norway.

Journal of Applied Polymer Science, Vol. 91, 2158–2167 (2004)

diffusion, in the particles. They found that diffusion in the polymer at the length scale of the particle diameter was the controlling transport mechanism. A possible explanation for the change in diffusion length scale in the polymer phase from the microparticles as assumed by the MGM, to a length scale on the order of the macroparticle, was suggested by McKenna and Mattioli.[6] They proposed a scheme for how the morphology evolved during polymerization. At low degrees of polymerization, a multigrain description is adequate with one catalyst fragment inside each of the grains building the macroparticle structure. As more polymer is formed, neighboring micrograins merge into larger structures with several catalyst fragments inside each. Thus, the length scale for mass transfer also changes.

The view of the multigrain structure is based on SEM and TEM photographs of nascent polymer particles such as those of Kakugo et al.[7,8] To visually detect the catalyst fragments on electron micrographs, it is necessary to use particles with a productivity as low as possible. Thus, the MGM is to a large extent based on observations of particles with low productivity. The work of Kakugo et al.[7,8] also indicates agglomeration of a few microparticles to what they call a polymer globule, which differs from the assumption of the MGM of only one catalyst fragment per microparticle. This agglomeration could be the first step in the agglomeration to larger structures. Their largest productivity (9 kg_{pol}/g_{cat}) is much lower than what is common in the industry today. Thus, the possible change in morphology at higher productivity is not thoroughly treated in the literature.

Another work that shows the need for a new look at mass-transfer scales is the work by Seland.[9] He examined the diffusion of toluene in industrially made polymer particles by an NMR technique, and found that the most appropriate way of describing the diffusion was in terms of three different diffusion coefficients varying by about two orders of magnitude. He interprets these results as three different "phases" within the particles, each with different diffusion properties. The largest diffusion coefficient, of the same order as the bulk diffusivity, is found in the macropores of the particle; the medium diffusivity comes from transport in mesoparticles, which are agglomerates of smaller particles; and the smallest diffusivity is found in the amorphous polymer surrounding the catalyst fragments.

The model presented in this work includes the effects of mass transfer at the levels described above. The main difference between the model presented in this work, compared to existing multilevel models, is the inclusion of a radial transport of monomer in the mesoparticle regions of the particle. As will be discussed later, the model may for a large number of particles also well represent cases with nonhomogeneous monomer concentration around the mesoparticles. The mass-transfer equations will be solved on a steady-state level. Thus we are not presenting a particle model that can simulate the whole process from the catalyst to the finished polymer particle. The model predicts only the mass-transfer properties, given the morphology.

THREE-LEVEL PARTICLE MODEL

The mesoscale as used in this work is typically 10–40% of the scale of the whole particle (macroscale). Figure 1 shows an example of a polymer particle and how to classify the length scales building up the morphology. As the figure illustrates, one particle can be considered to consist of mesoparticles, which in turn are made up of agglomerated microparticles with catalyst fragments inside. A typical size of the macroparticle is of the order 10–100 μm, the mesoparticle 1–10 μm, and the microparticles[7] 0.1 μm. The mass-transfer model presented in this work takes into account these different length scales.

Basic assumptions

Before going into details of the model, we limit the problem by introducing the following assumptions:

- The polymer particles and substructures are spherical and symmetrical; thus a one-dimensional model is appropriate.
- The analysis is stationary (the solution of the monomer concentration will be analogous to a dynamic model assuming pseudo steady-state).
- The particles are isothermal and there is no external boundary transfer resistance.
- The catalyst fragments are evenly distributed inside the mesoparticles. This is a simplification that allows us to use analytical solutions to the diffusion-reaction equations for calculating the local concentration of monomer.
- The microparticles are assumed to be much smaller than the mesoparticles; thus the mesoparticles can be treated as pseudo-homogeneous.
- The mass transport is by diffusion only and with constant diffusivities on the three scales. Convective effects as described in the work by Kittilsen et al.[10] are not considered.
- The reaction is first order with respect to monomer concentration.

The model equations

The general mass balance for component *i* in a system with mass transport and reaction is

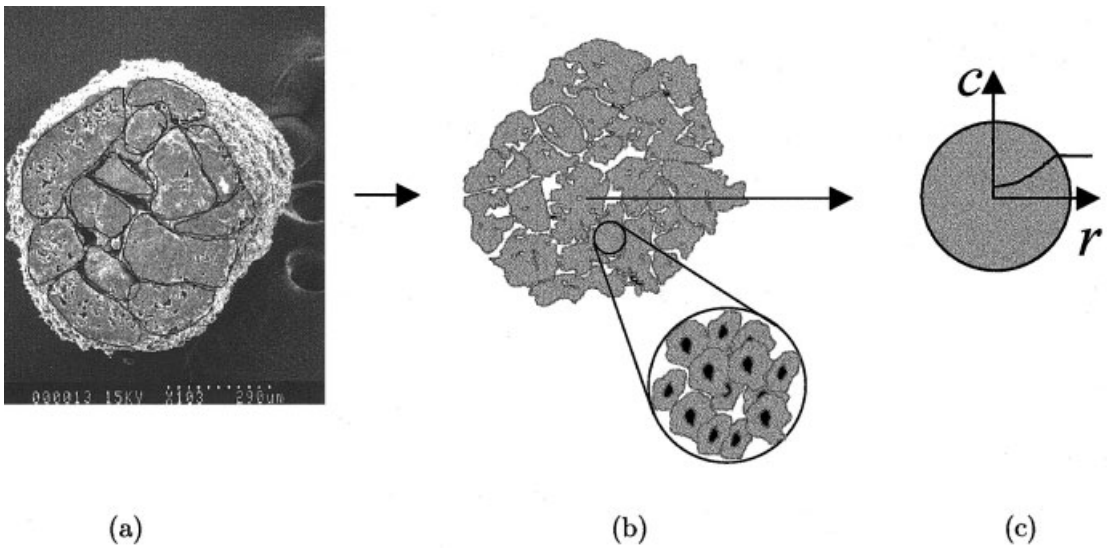

Figure 1 Morphology in a polymer particle can be classified into several levels. (a) SEM image indicating areas of mesoparticle level (here 20–30% of particle size). (b) Schematic of (a) together with a magnification showing microparticles and catalyst fragments (dark). (c) Possible variation in monomer concentration through a mesoparticle.

$$\frac{\partial c_i}{\partial t} + (\nabla \cdot N_i) = -R_i \tag{1}$$

Note that $R_i > 0$ means consumption of the species in this case. From now on only monomer, represented by M, will be considered. Mass transport is assumed to be by diffusion only (i.e., $N = -D\nabla M$). Then, for a symmetrical spherical particle at steady state (compare with the assumptions above), the mass balance becomes

$$-D\frac{1}{r^2}\frac{\partial}{\partial r}\left(r^2\frac{\partial}{\partial r}M\right) = -R \tag{2}$$

In the current model, we split the mass balance above into two equations (see Fig. 2): one for the monomer in the macropores and one for the monomer in the mesoparticles. Note that we here consider the radial transport of monomer on a macroscale of the particle. The monomer transfer between the two "phases" is set as a source term in the two equations

$$-D_M^g\frac{1}{r^2}\frac{\partial}{\partial r}\left(r^2\frac{\partial}{\partial r}M_M\right) = -F_{Mm} \tag{3}$$

$$-D_m^g\frac{1}{r^2}\frac{\partial}{\partial r}\left(r^2\frac{\partial}{\partial r}M_m\right) = +F_{Mm} - R \tag{4}$$

where subscripts M and m indicate macro and meso, respectively; superscript g indicates that the diffusivity is with respect to a global reference frame [see eq. (7) for more details]; and F_{Mm} is the volumetric rate of monomer transfer from macro to meso "phase."

Reaction occurs only in the mesoparticles, so this term is left out in the equation for the macroscale. Note that the reaction term unit is reaction rate per unit volume of macroparticle, not per unit of mesoparticle volume. A schematic representation of the monomer flow for this model is given in Figure 2.

Equations (3) and (4) have the entire particle as basis, and the available cross-sectional area for the two "phases" are taken care of by the effective diffusivities. Thus, the superscript g in the mesoparticle equation denotes global (whole particle). When the diffusive mass transport is mainly by pores, the common way to relate the effective diffusivity to the bulk dif-

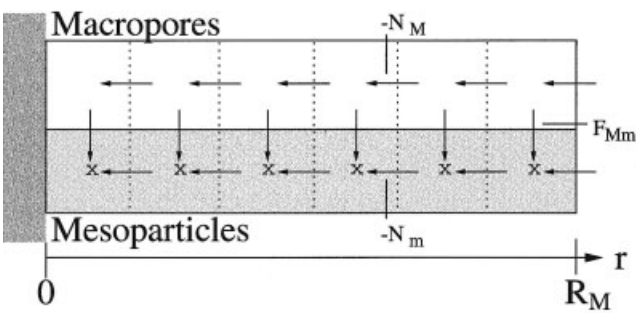

Figure 2 Schematic representation of the monomer flow in the current particle model. Flux of the monomer in the radial direction is indicated, N_m and N_M are the macropore and mesoparticle fluxes, respectively. Note the sign convention: a flux toward the particle center ($r = 0$) is a negative flux. The monomer transport from the macropores to the mesoparticles is given by F_{Mm} and has the sign convention as shown in the figure; the positive direction is from macropores to mesoparticles. This flow has units of mol per unit volume and time. "x" represents the reaction of monomer.

fusivity is through the porosity and tortuosity. The effective diffusivities in the macropores and in the mesoparticles are then

$$D_M^g = D_0 \frac{\epsilon_M}{\tau_M} \tag{5}$$

$$D_m = D_0 \frac{\epsilon_m}{\tau_m} \tag{6}$$

Here ϵ_M is the macroporosity and ϵ_m is the mesoporosity (i.e., the porosity in the mesoparticles). The diffusion of monomer in the mesoparticles will in general not only bring monomer to the active sites within the mesoparticles, but also contribute to the total radial transport in the macroparticle. When calculating this contribution to the "global" (i.e., macroparticle) mass transport, the effective diffusivity in the mesoparticles has to be adjusted for the mesoparticle's fraction of the total area. In a cross section of the particle, there will be a given area of macropores and a given area of mesoparticles. The area of macropores is already included through the macroparticle porosity ϵ_M in the effective macroparticle diffusivity. However, the global effective diffusivity in the mesoparticle, based on the total particle volume, must be corrected for the mesoparticles' volume fraction, corresponding to $1 - \epsilon_M$. Then, the effective global mesoparticle diffusivity is

$$D_m^g = (1 - \epsilon_M) D_m = D_0 \frac{\epsilon_m (1 - \epsilon_M)}{\tau_m} \tag{7}$$

Finally, we need a relationship between the mesoparticle monomer concentration and the macropore monomer concentration. The mesoparticles are assumed to be of spherical shape and with catalyst evenly distributed inside. If one solves the diffusion-reaction equation for this ideal system, it is possible to calculate a volume-averaged monomer concentration in the particle, and thus the effective reaction rate as Thiele did.[11] In this way we can link the monomer concentration in the macropore outside a mesoparticle with the average concentration inside the mesoparticle:

$$M_m = \eta_m M_M \tag{8}$$

where

$$\eta_m = \frac{3}{\phi_m^2} (\phi_m \coth \phi_m - 1) \quad \text{and} \quad \phi_m = R_m \left(\frac{k_p^{Vm}}{D_m} \right)^{1/2} \tag{9}$$

in which η_m is the mesoparticle effectiveness factor, R_m is the radius of the mesoparticles, and $k_p^{V_m}$ is a reaction rate constant per volume of mesoparticle. All these variables generally depend on the position in the macroparticle.

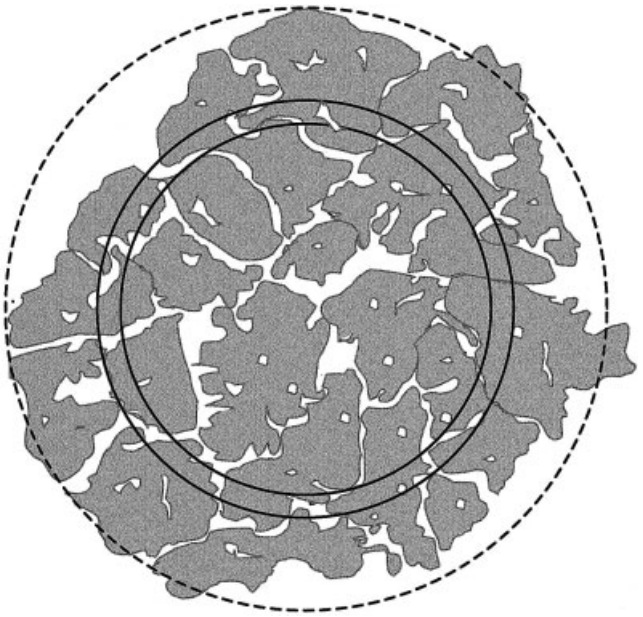

Figure 3 Illustration of how a volumetric average of the contents in the mesoparticles inside a shell will be equivalent to the average of a single mesoparticle. The outer dashed line represents the boundaries of the macroparticle. The two solid lines represent a shell, in which the monomer concentration inside the mesoparticles is the focus of interest.

The relationship between macropore and mesoparticle monomer concentration above needs to be justified. The model is one-dimensional; thus the values used for monomer concentration both in macro and meso phases are volume-averaged values of the contents of a shell in the spherical particle. Such a shell is illustrated in Figure 3. In reality the monomer concentration in the macropores may vary in a shell as the macrotortuosity and -porosity may vary if the mesoparticles are large. If the mesoparticles are small this will even out within individual polymer particles, whereas with large mesoparticles this may be envisaged as an average over a large number of polymer particles. The same goes for the mesoscale. The local concentration in the meso phase depends on the distance from the macropore, which depends on the size and shape of the mesoparticles. The shell cuts through various parts (inner, outer, middle) of mesoparticles and, averaged over many mesoparticles, an effectiveness factor based on the mesoparticle mean radius becomes reasonable. The approximations used above are believed to be fair as long as the size of the mesoparticle is not larger than 30–50% of the macroparticle.

The microparticle diffusion resistance is included using an effectiveness factor for the microparticle level. The derivation of this expression was done in the work by Floyd et al.,[1] and the result is

$$\eta_\mu = \frac{M_\mu}{M_m} = \frac{1}{1 + \frac{1}{3}\phi_\mu^2(\theta - 1)/\theta} \tag{10}$$

where

$$\phi_\mu = R_c\left(\frac{k_p^\rho \rho_c}{D_\mu}\right)^{1/2} \quad \text{and} \quad \theta = \frac{R_\mu}{R_c} \tag{11}$$

where μ indicates values at the microparticle level. R_μ and R_c are the microparticle radius and catalyst fragment radius, respectively; k_p^ρ is the propagation constant per unit mass of catalyst as basis; and ρ_c is the density of the catalyst. The relation between the propagation rate constant above and the one based on the mesoparticle volume [eq. (9)] is

$$k_p^{Vm} = \frac{P}{\rho_p(1 - \epsilon_m)}\, k_p^\rho \tag{12}$$

where P is the productivity (mass of polymer per mass of catalyst) and ρ_p is the density of polymer. To convert the reaction rate in terms of propagation rate per unit of particle volume, the following relation is used:

$$k_p^V = (1 - \epsilon_M)k_p^{Vm} \tag{13}$$

Using both the effectiveness factors at the microparticle and the mesoparticle levels, the reaction rate per volume of particle can be written as

$$R = k_p^V M_\mu = k_p^V \eta_\mu M_m = k_p^V \eta_\mu \eta_m M_M \tag{14}$$

Solving the set of equations

It is possible to obtain an analytical solution to the problem outlined above. By adding the mass transport equations in the two "phases," eqs. (3) and (4), one can eliminate the transport between the levels, F_{Mm}. Furthermore, by substituting $M_m = \eta_m M_M$ [eq. (8)] and inserting eq. (14) for the reactivity, one arrives at

$$-D_M^g \frac{1}{r^2}\frac{\partial}{\partial r}\left(r^2 \frac{\partial}{\partial r} M_M\right) - D_m^g \frac{1}{r^2}\frac{\partial}{\partial r}\left(r^2 \frac{\partial}{\partial r}\eta_m M_M\right) = -k_p^V \eta_\mu \eta_m M_M \tag{15}$$

If we now limit the investigation to cases where the mesoscale effectiveness factor η_m is independent of macroscale radial position, the equation can be written in the form

$$-(D_M^g + \eta_m D_m^g)\frac{1}{r^2}\frac{\partial}{\partial r}\left(r^2 \frac{\partial}{\partial r} M_M\right) = -k_p^V \eta_\mu \eta_m M_M \tag{16}$$

The boundary conditions are

$$r = 0, \quad \frac{\partial M_M}{\partial r} = 0 \tag{17}$$

$$r = R_M, \quad M_M = M_0 \tag{18}$$

where R_M is the radius of the macroparticle. The first boundary condition is a result of symmetry in the particle center and the last is a result of assuming no transport resistance to mass transfer from the bulk to the macroparticle surface. The macropore monomer concentration at the surface of the macroparticle is the same as the bulk monomer concentration M_0.

The resulting equation is the same type as solved by Thiele.[11] The solution is

$$M_M = M_0 \frac{R_M}{r}\frac{\sinh(\phi_M r/R_M)}{\sinh \phi_M} \tag{19}$$

where

$$\phi_M = R_M\left(\frac{\eta_\mu \eta_m k_p^V}{D_M^g + \eta_m D_m^g}\right)^{1/2} \tag{20}$$

The volume-average monomer concentration is found by integrating the equation above, which is[11]

$$\overline{M_M} = M_0 \eta_M = M_0 \frac{3}{\phi_M^2}(\phi_M \coth \phi_M - 1) \tag{21}$$

To find the average reaction rate, the above result is inserted into the rate equation [eq. (14)] to obtain

$$\bar{R} = k_p^V \overline{\eta_\mu \eta_m M_M} = k_p^V \eta_\mu \eta_m \eta_M M_0 \tag{22}$$

given that the microparticle and mesoparticle effectiveness factors are independent of the macroparticle radius. (This assumption is not necessarily good, and in a numerical solution, it can be avoided.) The total effectiveness factor is then

$$\eta_{\text{tot}} = \eta_\mu \eta_m \eta_M \tag{23}$$

where η_μ is given in eq. (10), η_m is given in eq. (9), and η_M is given in eq. (21). The microparticle diffusion resistance is normally neglected,[1] thus $\eta_\mu = 1$ has been used in the simulations below.

SIMULATIONS AND DISCUSSION

Base case

To illustrate the theoretical results, a base case calculation and a sensitivity analysis with variation in some of the parameters were done. The base case parameters used are listed in Table I. The monomer-specific parameters such as bulk diffusivity and concentration

TABLE I
Parameters Used in the Three-Level Particle Model

Parameter	Symbol	Base value	Unit
Activity	a	5	$kg_{pol}\ g_{cat}^{-1}\ h^{-1}$
Macroparticle radius	R_M	100	μm
Catalyst radius	R_0	20	μm
Mesoparticle size	R_m	$0.3R_M$	μm
Macroporosity	ϵ_M	0.2	—
Mesoporosity	ϵ_m	0.03	—
Macro tortuosity	τ_M	2	—
Meso tortuosity	τ_m	3	—
Bulk diffusivity	D_0	10^{-8}	m^2/s
Monomer bulk conc.	M_0	500	mol/m^3
Polymer density	ρ_p	900	kg/m^3
Catalyst density	ρ_c	2000	kg/m^3

were taken as typical values for olefins in a hydrocarbon solvent at moderate pressure (ethylene in heptane at pressure of 8 bar and temperature of 80°C using the Soave–Redlich–Kwong equation of state). To convert the activity in terms of mass basis to molar basis, the molecular weight of ethene was used. The macro- and mesoporosities and tortuosities are values set such that the diffusivities in the three levels (macro, meso, and micro) differ by a factor of 10 going from one scale to the other, in accordance with Seland's results.[9]

A simulation with the base case parameters gave both significant macro- and mesoscale diffusion limitations. The effectiveness factors at the two levels were $\eta_M = 0.71$ and $\eta_m = 0.58$, respectively. A plot of the monomer concentration as a function of macroparticle radius is given in Figure 4. The ratio of the mesoparticle concentration to the macropore concentration is constant and equal to the mesoparticle effectiveness factor $\eta_m = 0.58$.

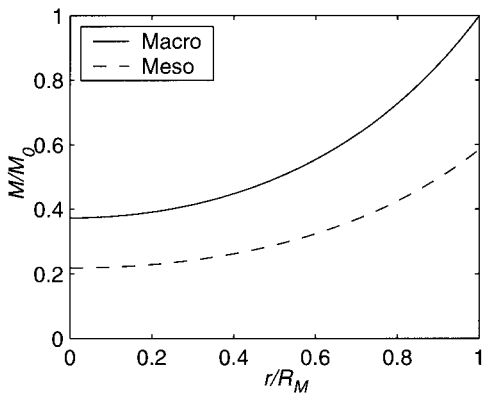

Figure 4 Average monomer concentration in the macro and meso phases as a function of radius as calculated by the base case parameters.

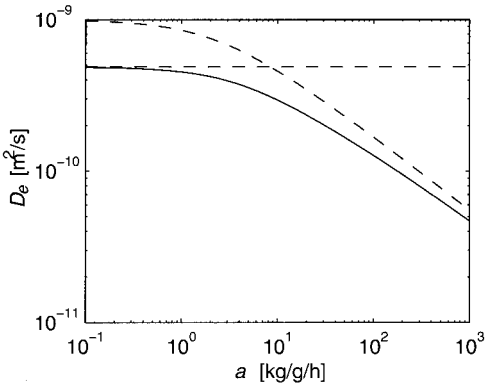

Figure 5 Effective diffusivity as a function of intrinsic activity. The dashed lines are the asymptotes.

Equivalent diffusivity

To compare with existing models, we will introduce an equivalent diffusivity corresponding to the diffusivity in an MGM or PFM model giving the same "observed" reaction rate as the one using the three-level particle model. Considering the particle as a pseudo-homogeneous medium with homogeneous distribution of the catalyst, a Thiele effectiveness factor can be used. From such a relationship the equivalent diffusivity D_e (Fig. 5) can be calculated:

$$\frac{3}{\phi_e^2}(\phi_e \coth \phi_e - 1) = \eta_e = \eta_{\text{tot}} \tag{24}$$

$$D_e = \frac{R_M^2 k_p^V}{\phi_e^2} \tag{25}$$

The total effectiveness factor is the product of the effectiveness factors (see Fig. 6) at the mesoscale level and at the macroscale level (when neglecting the microparticle diffusion resistance as we have done):

$$\eta_e = \eta_m \eta_M \tag{26}$$

Effectiveness factor one

The first case to study is what limit the equivalent diffusivity approaches as the effectiveness factors approach 1. The effectiveness factor at the mesoscale level and at the macroscale level are both functions of the Thiele modulus as given in eq. (24). Using the Taylor series $\coth(x) = 1/x + x/3 - x^3/45 + \ldots$, the effectiveness factor generally becomes

$$\lim_{\eta \to 1} \eta = \lim_{\phi \to 0} \eta = 1 - \frac{\phi^2}{15} \tag{27}$$

Inserting this result into eq. (26) gives

$$\left(1 - \frac{\phi_e^2}{15}\right) = \left(1 - \frac{\phi_m^2}{15}\right)\left(1 - \frac{\phi_M^2}{15}\right) \tag{28}$$

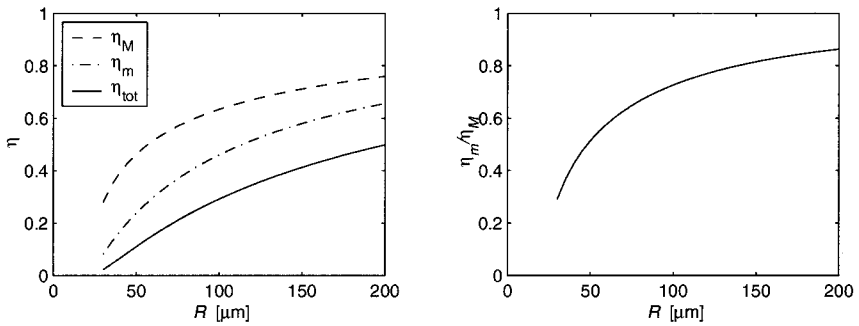

Figure 6 Effectiveness factors at the macroscale level (η_M) and mesoscale level (η_m), and the total effectiveness factor (η_{tot}) with varying the polymer particle radius. All other parameters such as activity and meso relative length scale were kept constant.

$$1 - \frac{\phi_e^2}{15} = 1 - \frac{\phi_m^2}{15} - \frac{\phi_M^2}{15} + \frac{\phi_m^2 \phi_M^2}{15^2} \tag{29}$$

and for ϕ_m and $\phi_M \ll 1$

$$\phi_e^2 = \phi_m^2 + \phi_M^2 \tag{30}$$

Inserting the expressions for the Thiele modulus yields

$$R_M^2 \frac{k_p^V}{D_e} = R_m^2 \frac{k_p^{Vm}}{D_m} + R_M^2 \frac{\eta_m k_p^V}{D_M^g + \eta_m D_m^g} \tag{31}$$

In this limit $\eta_m \to 1$, and by rearranging and inserting the relationship between the two propagation rate constants [eq. (13)] and the local to global mesoparticle diffusivity relationship [eq. (7)], the following estimate for the equivalent diffusion coefficient is found as the effectiveness factor η_m approaches 1:

$$\lim_{\eta_m \to 1} \frac{1}{D_e} = \frac{\left(\frac{R_m}{R_M}\right)^2}{D_m^g} + \frac{1}{D_M^g + D_m^g} \tag{32}$$

where we have used the relations $k_p^{Vm}/k_p^V = 1/(1 - \epsilon_M)$ and $(1 - \epsilon_M) D_m = D_m^g$.

Effectiveness factor zero

The other limit to study is when the effectiveness factor approaches 0. Then the general effectiveness factor is

$$\lim_{\eta \to 0} \eta = \lim_{\phi \to \infty} \eta = \frac{3}{\phi} \tag{33}$$

and eq. (26) now yields

$$\frac{3}{\phi_e} = \eta_m \frac{3}{\phi_M} \tag{34}$$

$$\frac{1}{\phi_e^2} = \eta_m^2 \frac{1}{\phi_M^2} \tag{35}$$

Inserting the equations for the Thiele modulus for the effective and macroparticle terms yields

$$\frac{1}{R_M^2} \frac{D_e}{k_p^V} = \eta_m^2 \frac{1}{R_M^2} \frac{D_M^g + \eta_m D_m^g}{\eta_m k_p^V} \to \eta_m^2 \frac{1}{R_M^2} \frac{D_M^g}{\eta_m k_p^V} \tag{36}$$

$$\lim_{\eta \to 0} D_e = \eta_m D_M^g = 0 \tag{37}$$

As an illustration of the above results, a set of simulations were run where the intrinsic activity was varied from 0.1 to 1000 kg g^{-1} h^{-1} to see both limits. The effective diffusivity as a function of activity is plotted in Figure 5. As the activity approaches 0, the effectiveness factors approach 1 and the effective diffusivity moves to the limit as described in eq. (32), which in this case is $D_e = 4.9 \times 10^{-10}$ m^2/s. As the intrinsic activity is raised to large values, the other limit for the effective diffusivity as described in eq. (37) is approached.

Effect of particle growth on diffusion characteristics

As the virgin catalyst particle turns into a polymer particle, increasing its size tenfold, the conditions for the diffusion of monomer into the particle also change radically. Obviously, the length scale for diffusion increases, which in itself should give a more pronounced diffusion resistance to the reaction rate. However, because the produced polymer "dilutes" the catalyst fragments, the volumetric reaction rate decreases. The overall effect of the particle growth is

that the diffusion resistance decreases (the effectiveness factor increases).

Consider the case where there is no agglomeration of mesoparticles; thus the mesoparticle size is constant relative to the macroparticle size. In this case, both the macro and the meso effectiveness factors will increase with the production of polymer (i.e., with increasing the polymer particle size). This is illustrated in Figure 6, using the base case parameters (Table I), and calculating the two effectiveness factors for different particle sizes. Both effectiveness factors increase with polymer production. The fraction η_m/η_M is in the range 0.2–0.8, meaning that both of the factors are important when determining the total effectiveness, but also indicating that the diffusion resistances at the macro- and mesoscales change somewhat differently. The mesoscale effectiveness factor is more dominating in the early stages of the polymerization (for small R).

As discussed in the introduction, several studies indicate an internal agglomeration of substructures in a growing polymer particle during growth. This will change the relative length scales of the meso- and macroscales. The formation of larger mesoparticles will give a more severe diffusion limitation on this scale. The effect of reduced effectiveness attributed to agglomeration during growth "competes" with the dilution effect discussed above. Whether the result is an increased diffusion resistance depends on the rate of agglomeration. To answer that question, an agglomeration model is needed that is beyond the scope of this work.

Path of monomer transport

Another important problem that can be investigated with this model is what path the monomer takes from the bulk phase to the active sites. Intuitively, one might guess that the monomer mainly follows the larger pores in the particle. However, because this model also allows for mass transport in the mesoparticles to contribute to the macroparticle radial transport, it is of interest to see how much this transport contributes to the total.

The quantities to compare are the macro to meso transfer F_{Mm} and the reactivity R. The schematic representation of the particle as shown in Figure 2 shows that the mass balance in the mesoparticle is a result of the inflowing monomer from the macropores, the net change in mesoparticle flux, and finally reaction. It means that the fraction of F_{Mm} to R tells how much of the reacting monomer comes from the macropores.

Using the relation between macropore concentration and mesoparticle concentration [eq. (8)], it is possible to find the fraction of F_{Mm} and R from the mass balances [eqs. (3) and (4)]:

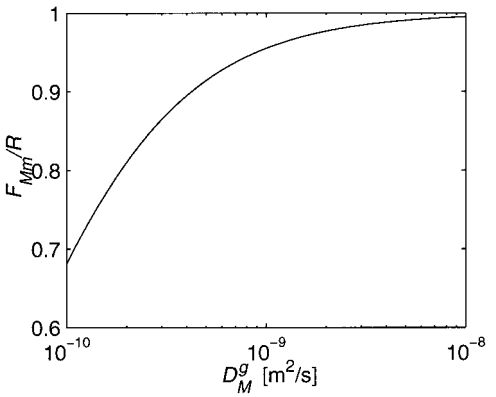

Figure 7 Fraction of the monomer reaction that comes from transport in the macropores as a function of macropore effective diffusivity.

$$\frac{F_{Mm}}{R} = \frac{1}{1 + \dfrac{\eta_m D_m^g}{D_M^g}} \tag{38}$$

Using the base case parameters, this relation yields $F_{Mm}/R = 0.96$. Thus, most of the monomer is transported along the macropore "highways" of the particle before exiting near the active sites. A further study of the variation of this quantity with macropore diffusivity is shown in Figure 7. Here the macropore diffusivity D_M^g was varied from 10^{-10} to 10^{-8} m^2/s (10^{-9} m^2/s is the base case value) keeping the mesoparticle diffusivity constant. As expected, the higher the diffusivity in the macropores, the larger the fraction of the monomer using the path by the macropores. At $D_M^g = 10^{-8}$ m^2/s almost all the transport of monomer is in the macropores. In this case the ratio of macro to meso diffusivity is so large ($\sim$100), that the radial transport in the particle is almost solely provided by the macropore diffusion, and the mesoscale diffusion is only a transport mechanism from the macropores to the active sites.

Importance of the meso level

We have seen the effects of introducing the three-level particle model above, but we have not explicitly discussed when this model should be used instead of a traditional MGM or PFM (polymer flow model; i.e., with only one scale of diffusion limitation).

In the MGM and PFM, the mesoparticle diffusivity is either neglected or an integrated part of the macroscale diffusivity. The meso level is important when the mesoparticle effectiveness factor is significantly lower than 1, as we have seen in the preceding sections. The Thiele modulus at the mesoscale level can be rewritten as

$$\phi_m = R_m\left(\frac{k_p^{Vm}}{D_m}\right)^{1/2} = \left(\frac{R_m}{R_M}\right)R_M\left(\frac{k_p^V}{D_m^g}\right)^{1/2} = \left(\frac{R_m}{R_M}\right)\phi'_M \tag{39}$$

where ϕ'_M is the Thiele modulus one would have if the effective diffusivity in the macroparticle was D_m^g. We can use this relationship directly to identify the important parameters that determine when the three-level particle model should be used. First, the mesoparticle size should be a significant fraction of the total particle size; second, the Thiele modulus ϕ'_M should be significantly greater than 1. However, at the risk of overgeneralizing, we will try to define a more specific criterion by comparing the Thiele modulus at the meso level with that on the macroscale [eq. (20)]:

$$\frac{\phi_m}{\phi_M} = \frac{\left(\frac{R_m}{R_M}\right)R_M\left(\frac{k_p^V}{D_m^g}\right)^{1/2}}{R_M\left(\frac{\eta_m k_p^V}{D_M^g + \eta_m D_m^g}\right)^{1/2}} = \left(\frac{D_M^g + \eta_m D_m^g}{\eta_m D_m^g}\right)^{1/2}\left(\frac{R_m}{R_M}\right) \tag{40}$$

A conservative approach is to set $\eta_m = 1$. A smaller η_m will lead to a larger ϕ_m and thus smaller R_m required for the mesoscale to be important. The other simplification is to set a typical value for the ratio D_M^g/D_m^g of approximately 10 as in the base case. Inserting these simplifications, the above equation yields

$$\phi_m \approx \sqrt{10}\left(\frac{R_m}{R_M}\right)\phi_M \approx 3\left(\frac{R_m}{R_M}\right)\phi_M \tag{41}$$

Thus as a rule of thumb, as the macroscale diffusion resistance starts to become significant ($\phi_M > 1$), the meso length scale should be approximately 1/3 of the macro length scale for the mass-transfer resistance at the meso level to be significant ($\phi_m > 1$). However, as the mass-transfer limitations at the macroscale become more severe ($\phi_M \gg 1$) (i.e., for lower diffusivities or higher activities), a smaller mesoparticle size will give significant mass-transfer resistance at the mesoparticle level. This is illustrated in Figure 8 where R_m/R_M is plotted as a function of intrinsic activity for the criterion that mesoscale mass-transfer resistance becomes significant ($\phi_m = 1$). The base case parameters are used for all except the activity. For instance, given the base case parameters with $a = 5$ kg g^{-1} h^{-1}, the critical R_m is approximately $0.1R_M$, meaning that the base value $R_m = 0.3R_M$ is above the critical value, so the mass-transfer resistance at the mesoparticle level will be significant and should be included.

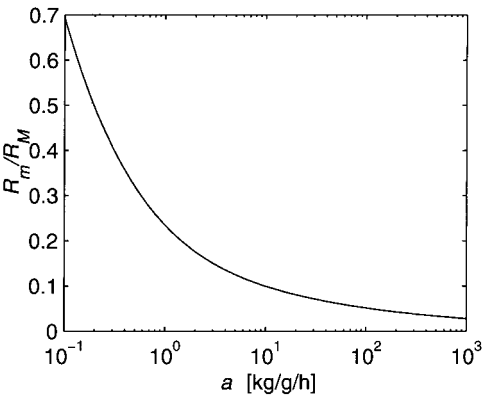

Figure 8 Critical mesoparticle size as a function of activity given the base case parameters. For combinations of the parameters a and R_m/R_M above the curve, the mass transfer resistance at the meso level will be significant and should be included in the model.

CONCLUSIONS

A new mass-transfer model to be used in single-particle models for olefin polymerization, the three-level particle model, has been presented. The difference between this and traditional single-particle models is the introduction of a third level of morphology, the meso level, with a length scale between the size of the microparticles and the size of the whole particle. The polymer particles can be regarded as composed of agglomerates of mesoparticles, with the size of some tenths of the size of the whole particle. The model presented here can account for a variable monomer concentration around these mesoparticles and can estimate the influence these have on the total mass transfer in the particles.

The three-level model presented here also helps us to understand the influence of particle morphology and reaction rate on the value of an effective diffusion coefficient that could be used in a traditional MGM/PFM model. Such a coefficient would give us equivalent rates and concentration gradients. The model described here helps to quantify effects that cannot be accounted for in the MGM.

The model shows that given typical parameters, the main path for mass transport in the particles is a radial diffusion in the macropores and then diffusion in a tangential direction to the active sites at the mesoparticle level. The mesoscale level contributes only to a small fraction of the total radial mass transport.

As a rule of thumb, the introduction of the meso level in single-particle models should be considered when the macroscale diffusion resistance becomes important and the meso length scale is about 30% of the macro length scale. For more severe macroscale diffusion resistance, even smaller mesoparticles can induce significant effects.

Meanings and Units of Abbreviations and Symbols

Abbreviation or symbol	Meaning	Unit
EPR	Ethylene–propylene–rubber	
MGM	Multigrain model	
NMR	Nuclear magnetic resonance	
PFM	Polymer flow model	
SEM	Scanning electron microscopy	
TEM	Transmission electron microscopy	
a	Activity	$kg_{pol}\ g_{cat}^{-1}\ h^{-1}$
c_i	Concentration of component i	mol/m^3
k_p^ρ	Propagation constant, mass catalyst basis	$(m^3/mol)^n\ mol\ kg^{-1}\ s^{-1}$
k_p^V	Propagation constant, volume basis	$1/s$
r	Radial position in particle	m
D	Diffusion coefficient	m^2/s
D_e	Equivalent diffusion coefficient	m^2/s
D_m	Effective diffusivity in meso "phase"	m^2/s
D_M^g	Effective global diffusivity in macro "phase"	m^2/s
D_m^g	Effective global diffusivity in meso "phase"	m^2/s
D_μ	Diffusion coefficient in microparticle (i.e., in polymer)	m^2/s
F_{Mm}	Volum. rate of monomer transf. from macro to meso "phase"	$mol\ m^{-3}\ s^{-1}$
M_0	Equilibrium monomer concentration	mol/m^3
M_m	Monomer concentration in meso "phase"	mol/m^3
M_M	Monomer concentration in macro "phase"	mol/m^3
M_μ	Monomer concentration at catalyst fragment surface	mol/m^3
N_i	Molar flux of component i	mol/m^2s
P	Productivity	kg/g *or* kg/kg
R	Volumetric reaction rate	$mol\ m^{-3}\ s^{-1}$
R_0	Catalyst initial radius	m
R_i	Volumetric reaction rate of component i	$mol\ m^{-3}\ s^{-1}$
R_m	Mesoparticle radius	m
R_M	Macroparticle radius	m
ϵ_m	Mesoparticle porosity	
ϵ_M	Macroparticle porosity	
η_i	Effectiveness factor at level i	
ϕ	Thiele modulus	
ρ_c	Catalyst density	kg/m^3
ρ_p	Density of polymer	kg/m^3
τ_M	Macroparticle tortuosity	
τ_m	Mesoparticle tortuosity	
θ	Growth factor microparticle	

The authors thank the Norwegian Research Council (NFR) under the Polymer Science Program for financial support of this work.

References

1. Floyd, S.; Choi, K. Y.; Taylor, T. W.; Ray, W. H. J Appl Polym Sci 1986, 32, 2935.
2. Kittilsen, P.; McKenna, T. F. J Appl Polym Sci 2001, 82, 1047.
3. Skomorokhov, V. B.; Zakharov, V. A.; Kirillov, V. A.; Bukatov, G. D. Polym Sci USSR 1989, 31, 1420.
4. McKenna, T. F.; Schweich, D. Dechema-Monogr 1992, 127, 169.
5. Sliepcevich, A.; Storti, G.; Morbidelli, M. J Appl Polym Sci 2000, 78, 464.
6. McKenna, T. F.; Mattioli, V. Macromol Symp 2001, 173, 149.
7. Kakugo, M.; Sadatoshi, H.; Sakai, J.; Yokoyama, M. Macromolecules 1989, 22, 3172.
8. Kakugo, M.; Sadatoshi, H.; Sakai, J. In Morphology of Nascent Polypropylene Produced by $MgCl_2$ Supported Ti Catalyst; Keii, T.; Soga, K., Eds.; Catalytic Olefin Polymerization; Elsevier: Amsterdam/New York, 1990; pp 345–354.
9. Seland, J. G. Ph.D. Thesis, NTNU, Trondheim, Norway, 2000.
10. Kittilsen, P.; Svendsen, H.; McKenna, T. F. Chem Eng Sci 2001, 56, 3997.
11. Cussler, E. L. Diffusion. Mass Transfer in Fluid Systems; Cambridge University Press: New York, 1984.